

Unraveling Mediaeval human traces in fluvial deposits of the Dyje River near the Pohansko stronghold (Czech Republic)

Slavomír NEHYBA¹*, Katarína ADAMEKOVÁ¹, Nela DOLÁKOVÁ¹, Petr DRESLER²,
Jan PETŘÍK¹ and Michaela PŘIŠŤÁKOVÁ²

¹ Masaryk University, Faculty of Science, Department of Geological Sciences, Kotlářská 2, CZ- 611 37 Brno, Czech Republic

² Masaryk University, Faculty of Arts, Department of Archaeology, Czech Republic



Nehyba, S., Adameková, K., Doláková, N., Dresler, P., Petřík, J., Příkladková, M., 2023. Unraveling Mediaeval human traces in fluvial deposits of the Dyje River near the Pohansko stronghold (Czech Republic). *Geological Quarterly*, 2023, 67: 48; <http://dx.doi.org/10.7306/gq.1718>

Sedimentological, archaeological, geochemical and pollen analyses combined with numerical dating were employed to examine the fluvial deposits of the Dyje River within the immediate vicinity of the Pohansko stronghold (Moravia, Czech Republic). This comprehensive approach facilitated the reconstruction of the chronology and nature of the processes in both the Dyje River catchment and its floodplain, mostly during the Medieval period. The older overbank deposits accumulated during the Late Holocene sometime before the 9th century CE. Palaeochannel sands were deposited between the 9th and 11th centuries CE as the infill of one fluvial channel of the Dyje River. The lower part of these sands displays direct traces of human intervention, including stones interpreted as from pavements and a wooden construction dated between 894 and 914 CE. The wooden construction may represent the remains of a bridge, a device for fish capture or a wooden structure. Geochemical signals associated with human activities are elevated in the palaeochannel sands, in part contemporary with the settlement activities at the Pohansko stronghold. Anthropogenic pollen indicators indicate the highest intensity of agriculture in the river catchment also in this period. After abandonment of the channel, the younger upper overbank deposits accumulated after the 11th century CE.

Key words: fluvial archive, palaeochannel sands, human activity, geoarcheology, numerical dating, environmental reconstruction.

INTRODUCTION

Fluvial archives represent the main component of the continental sedimentary record at any time (Miall, 2006), providing data about regional topography, palaeoclimate, discharge characteristics, base level changes, sediment supply, and so on (Colombera and Mountney, 2019). Fluvial deposits are responsive to many environmental forcing factors. Climate represents the most significant allogenic factor affecting fluvial deposits during the Quaternary period, as it modifies the environment of the catchment area (e.g., vegetation cover, discharge, sediment supply), which controls basic river characteristics, sedimentation style and rate of erosion (Vandenberghe, 1993, 2008, 2003; Vandenberghe et al., 1994; Mol et al., 2000; Houben, 2003; Leigh, 2006; Macklin et al., 2012). However, the increasing role of anthropogenic forcing on processes and de-

position within river catchments in the Holocene make the situation yet more complicated (Brooks, 2003; Hoffmann et al., 2009; Notebaert and Verstraeten, 2010; Lewin and Macklin, 2010; Erkens et al., 2011; Brown et al., 2018; Candel et al., 2018; Vayssière et al., 2019). Therefore, Holocene fluvial deposits can provide unique information on both natural and anthropogenic processes in fluvial catchments and also attest to the evolution of the depositional environment and variations in human settlement on floodplains.

Efforts to distinguish between autogenic and allogenic ruling factors, combined with evaluation of human influence, have been the focus of many studies (Erkens et al., 2011; Kadlec et al., 2015; Brown et al., 2018). However, each river system is different and shows specific behaviours (Notebaert et al., 2018; Elznicová et al., 2021). Human pressure on fluvial landforms and the environment is considered as a complex nonlinear process starting in the Neolithic Age (Lespez et al., 2007; Brown et al., 2013; Notebaert et al., 2018). Deforestation and agricultural activities increase rates of erosion and deposition within floodplains (Opravil, 1983; Rulf, 1994). Constructional activities and hydraulic engineering works have affected river courses, stream power, rate and type of erosion and amount and quality of transported material since the Medieval Age. All these processes are reflected in decreases in landscape and habitat diversity.

* Corresponding author, e-mail: slavek@sci.muni.cz

Received: June 6, 2023; accepted: October 10, 2023; first published online: January 30, 2024

Here, we present a multidisciplinary study (based on sedimentology, geochemistry, pollen analyses, archaeology, optically stimulated luminescence/OSL, radiocarbon dating and dendrochronology) of the deposits of the Dyje River (a lowland sinuous river) that accumulated in close proximity to the Early Mediaeval fortified site of Pohansko, and link their variations to the climatic and/or anthropogenic context. The study:

- identified conditions of deposition of the deposits studied, especially the sedimentary infill of the fluvial palaeochannel;
- reconstructed the natural processes within the river catchment for a particular time span;
- evaluated the role of natural and human factors on the Dyje River sedimentation during the Middle Ages.

REGIONAL SETTING

The area under study is located within the extended floodplain of the Dyje/Thaya River in the southeastern corner of the Czech Republic (South Morava region), close to the border with Austria. The Dyje River drains an area of 13,419 km² in the southeastern part of the Czech Republic and northern Austria. Its confluence with the Morava/March River is located ~15 km SE of the study area. Upstream of the confluence, the floodplain has the character of a flat 3–8 km wide lowland with numerous lateral channels. Its altitude varies between 155 and 157 m a.s.l.

The area studied is situated in the forefield of the western bailey of the Early Medieval fortified site of Pohansko (Fig. 1). The sediments were studied in an artificial trench excavated in 2017 (trench I) and reopened in the spring of 2020 (trench II). The position of the trenches is illustrated in Figure 1. The trenches extended from the destruction of the rampart towards the Dyje channel, and gradually expanded in the area of the riverbed to an area of 18 m².

GEOLOGICAL SETTING

The area is located within the Neogene Vienna Basin, which is filled with marine to brackish deposits (Eggenburgian to Pannonian in age) (Jiříček and Seifert, 1990). Grey clays (Pannonian) with a highly irregular top represent the direct bedrock of the extensive Late Pleistocene and Holocene deposits.

Late Pleistocene and Holocene sands and sandy gravels accumulated in the last 22,400 years (Havlíček, 2004). The fluvial deposits show considerable grain-size variations, and were deposited as infills of fluvial channels, and levee and overbank deposits. The fluvial channels were relatively shallow and broad (high width/depth channel ratio) with a meandering pattern (Petřík et al., 2019). They recently yielded OSL (optically stimulated luminescence) ages of 13.5, 11.8 and 10.3 ky BP (Nehyba et al., 2018). These fluvial deposits are locally overlain by (or rarely interfinger with) Late Pleistocene sand dunes. These dunes locally protrude directly at the surface, forming the sandy elevations called hrůd. They are interpreted as wind-blown dunes with sand eroded from fluvial deposits at the end of the Pleistocene and in the Early Holocene (Havlíček et al., 2016). However, some of these elevations seems to be fluvial in origin (Nehyba et al., 2018). Moreover, the presence of Mesolithic artefacts and subfossil soils within these sands points to their complicated Holocene evolution, including phases of both fluvial and aeolian redeposition and phases of pedogenesis (Havlíček and Smolíková, 2002; Petřík et al., 2019).

The fluvial and aeolian sands are mostly buried under younger greyish-black sandy or clayish loams and channel deposits (Petřík et al., 2019). The onset of flood loam deposition is estimated to be about 4.0–3.0 ky BP (Late Holocene) according to the oldest radiocarbon ages (Havlíček, 2001, 2004), which accords with palynological and archaeobotanical data (Opravil, 1983; Havlíček and Smolíková, 2002; Břízová and Havlíček, 2002; Havlíček, 2004; Doláková et al., 2010). The sedimentary infill of the fluvial channels has been dated to the 8th–3rd century BC (Petřík et al., 2019).

Enhanced flood loam sedimentation is inferred after the decline of the Great Moravian Empire in the 10th century AD (Opravil, 1983) because the youngest flood deposits overlie the destroyed and abandoned remains of the Great Moravian rampart (Macháček et al., 2007). The numerical age of these deposits, though, is still unknown, and they might belong to the High Middle Ages or the Modern Age (Dresler, 2016). Overbank deposits locally accumulated as late as the 15th century CE (Petřík et al., 2019). Their deposition was not continuous as they are intercalated with buried soil horizons (Macháček et al., 2007; Adameková et al., 2022). Geological and pedological maps of the area under study can be seen in Figure 1.

ARCHAEOLOGICAL CONTEXT

The area of the Dyje floodplain studied in the vicinity of Pohansko was inhabited only sporadically until the 9th century. Settlement is documented from the Mesolithic to the end of the Roman period (400 CE) by rare finds of objects. In the second half of the 6th century, the area was inhabited by early Slavs. According to dendrochronological data from wells and the rampart, the construction of the fortified Great Moravian centre at Pohansko began in the second half of the 9th century (Dresler, 2016). Archaeological and geophysical research has reconstructed an organized and dense settlement with evidence of craft and agricultural activities (Dresler and Beran, 2019; Prištáková and Milo, 2021).

The densely populated centre was almost entirely abandoned during the first quarter of the 10th century. Artefacts and settlement activities were recorded only in the former north-eastern suburb and at the newly settled site of Na včelách. In both cases, these were small settlements whose economy was apparently focused on beaver hunting (Dresler et al., 2022). The last evidence of settlement in the area dates back to the 11th century, when the stone church of the Great Moravian Manor was briefly used as a dwelling. Since the 11th century, there was establishment of settlements and villages outside the floodplain, in the wider area of the former centre (Dresler, 2016). The geopolitical development of the wider area transformed the core territory of the Great Moravian entity (10th century) into a border zone between Moravia/the Duchy of Bohemia and Austria/the Duchy of Austria. Until the beginning of the 19th century, the area of the former Great Moravian centre was used only as a hunting ground and exploited for wood and stone, taken as the rampart was dismantled (Dresler, 2016; Doláková et al., 2020).

METHODS

Lithofacies analysis was based on detailed bed-by-bed logging (Tucker, 1988; Walker and James, 1992) and evaluation of primary sedimentary structures and textures. Sieving and laser methods were combined for grain-size analysis (7 samples).

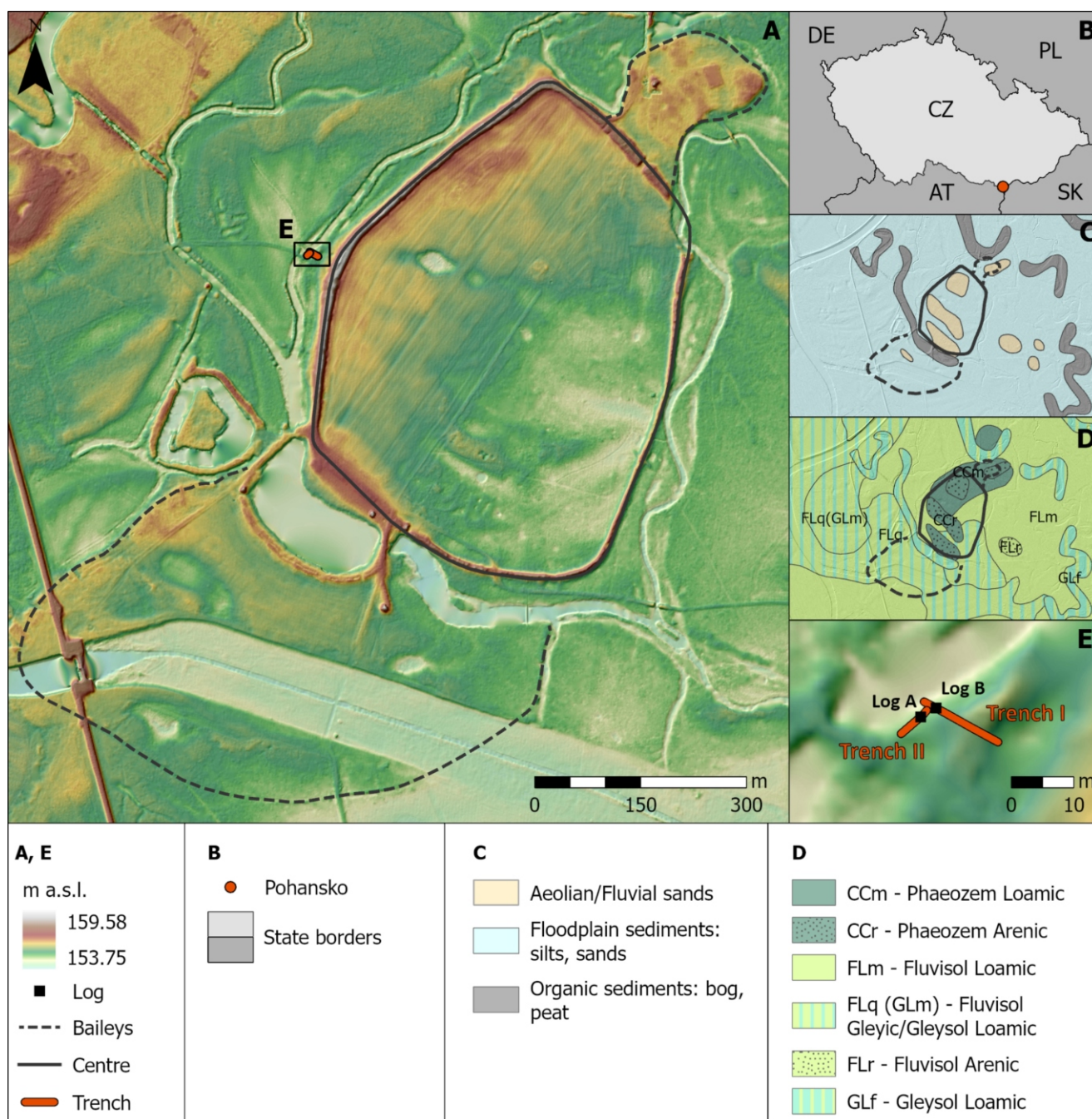


Fig. 1. Geographic location of the study area

A – digital elevation model based on LiDAR data for the area with the geographic position and the positions of trenches;
B – location of the study area within Central Europe; **C** – geological map of the study area; **D** – pedological map of the study area;
E – detailed positions of trenches and logging sites

A *Retsch AS200* sieving machine analysed the coarser fraction (4–0.063 mm, wet sieving). A *Cilas 1064* laser diffraction granulometer was used for analyses of the finer fraction (0.0001–0.5 mm). Ultrasonic dispersion, distilled water and washing in sodium polyphosphate were applied prior to analyses in order to avoid flocculation of the particles analysed. Grain size characteristics were counted according to [Folk and Ward \(1957\)](#).

Chemical composition was determined on a *Rigaku NexCG* energy-dispersive fluorescence spectrometer (ED-XRF), equipped with a *50-W Pd* tube and an SSD detector of 145-eV resolution. This device used indirect excitation by secondary targets

to improve signal-to-noise ratio. Thirty eight bulk samples (with 20 cm vertical resolution in the upper part of the section and 5 cm vertical resolution from 80 cm depth) were dried and cleared of organic material (roots, branches etc.) and stone fragments. Then the samples were homogenized and powdered in a *Retsch PM 100* agate planetary mill. Finally, the samples as pressed pellets were analysed. The time of excitation was 120 seconds for each target. Matrix-matching calibration was done according to international reference materials and standards (e.g., GBW 07406, GBW 07103, SARM42, JSO1, DC 61101, GBW 03103, GBW 03101a, GBW 03102a, DC 78302,

SRM2709a, BCR723, Metranal-31, Metranal-33, ERM-CC020, BAM-U110, NIST679, SM9939). From the resulting dataset, only concentrations of P, S, Ca, Ni, Cu, As and Pb expressed in parts per million (ppm) are discussed below. These elements may be associated with human activities (cf. Bintliff and Degryse, 2022).

Five samples for OSL dating were taken by standard procedure into steel tubes with 5 cm in diameter, directly from the trench walls to prevent daylight irradiation. Four samples were collected from Log A, while the fifth sample, X, was taken from Log B and its position is almost identical with the position of sample 1 (see Nehyba et al., 2020). Dating of quartz was carried out at the GADAM Centre (lab. Code GdTL) of the Silesian University of Technology in Gliwice (Moska et al., 2021). One wood fragment (D18) was analysed in the dendrochronological laboratory in Mikulčice of the Institute of Archaeology of the Academy of Sciences in Brno, processed using standard dendrochronological methodology (Cook and Kairiukstis, 1990).

For palynological purposes, samples were laboratory processed using the standard Erdtman method (Erdtman, 1960): HCl, HF, KOH and acetolysis [$\text{H}_2\text{SO}_4 + (\text{CH}_3\text{CO})_2\text{O}$]. Due to increased palynomorph numbers in sediment with low organic content, heavy liquid ZnCl_2 was employed. Palynomorphs were determined using a Nikon Alphaphot 2 optical microscope, largely after Van Geel et al. (1983), Reille (1995), Komárek and Jankovská (2001) and Beug (2004). The pollen diagram was processed using the POLPAL programme (Walanus and Nalepka, 1999).

RESULTS

SEDIMENTOLOGY AND ARCHAEOLOGY

The lithofacies of the succession studied are summarized in Table 1 and organized into four facies associations. The positions of lithological logs are illustrated in Figure 2 and the logs with the distribution of facies and facies associations are shown in Figure 3. Facies associations (FAs) are for simplicity labelled with interpretive genetic names, but their descriptions are separated from interpretations in the text. These FAs are:

- floodplain deposits (FA 1);
- artificial pavement and wood constructions at the bottom of the palaeochannel (FA 2);
- fluvial channel deposits (FA 3);
- floodplain deposits affected by pedogenesis (FA 4).

Logs, examples of lithofacies, and line drawings illustrating the distribution of facies associations in logs are shown in Figures 3A, B, 4A–E and 5A–E. Grain size data show lithological differences between recognised FAs (Figs. 6 and 7).

FA 1 consists of monotonous beds of facies M1 forming the basal part of the sedimentary succession studied (Fig. 3A, B). Sandy silts to clayey silts of facies M1 reveal a highly irregular erosive concave-down top. The content of silt is 56.5%, of the sand fraction is 34.6% and of clay is 8.9%. The average grain size (mean) is 5.0Φ (coarse silt) while the standard deviation

Table 1

Descriptive summary list of lithofacies of the deposits distinguished at the Pohansko locality

Symbol	Description	Interpretation
Ga	Isolated cobbles and rare boulders. Mainly limestones or sandy limestones with disc or blade shape, mostly subrounded. Preferred orientation with A–B plane oriented horizontally (parallel to surface). Commonly also presence of various wood fragments. Discontinuous occurrence of this facies and highly variable thickness ("one clast thick").	Evidence of human activity – clasts represent artificial pavement on the bottom of the fluvial channel. Wood construction of unknown purpose(s).
Gm	Pebble gravel, dominantly clast-supported, less commonly matrix-supported (upwards in the bed) – sandy matrix. Poorly sorted. Pebbles (quartz, gneiss) mostly rounded to subrounded, up to 6 cm in diameter. Irregular wedge-shaped bed; its thickness varies from 15 cm to isolated single pebbles over a distance of 3 m (thinning generally in direction to E). Sharp erosive concave-down base. Irregular sharp undulose top.	Fluvial deposits, base of the fluvial channel, channel "lag" (Miall, 2006), or inudite <i>sensu</i> Durand (2006).
Sr	Fine, medium, medium- to coarse-grained sand, ripple cross-stratified, micaceous. Relatively well-sorted with very rare occurrence of isolated granules to small pebbles. Set thickness of 6 cm. Cosets up to 20 cm with a fining upwards trend. Broadly wedge-shaped beds thinning towards the E. Sharp concave-down base, irregular undulose to convex-up top.	Tractional deposition, upper part of the lower flow regime, migration of bedforms as 3D ripples. Aggradation of fluvial dunes/bars (Best, 1996; Miall, 2006).
Sl	Fine, medium, medium- to coarse-grained sand, plane parallel lamination mostly horizontal to low inclination. Relative well-sorted. Tabular beds up to 15 cm thick. Sharp flat to undulose base. Top commonly sharp, but gradual transition upwards into facies Sm also observed.	Tractional deposition, upper-stage flow condition/higher fluvial discharge, top part or overflow of the fluvial dune/bar (Miall, 2006).
Sm	Fine, fine- to medium-grained sand, structureless/massive. Relative well-sorted. Tabular beds up to 10 cm thick. Transitional base from facies Sl, sharp erosional broadly convex-down top.	Rapid deposition from high-energy turbulent suspension, decelerating flow, rapid (Miall, 2006; Zieliński and Widera, 2020).
Fl	Very fine sand, silty sand to sandy silt. Planar parallel lamination locally disturbed by roots. Relatively well-sorted. Recognized both as tabular medium thick beds and as irregular lensoidal beds with thicknesses up to 5 cm and lateral extents of max. 1 m. Sharp irregular bases, mostly erosive tops (if facies Sr or Sl in superposition), but gradual transitional tops if facies M2 in superposition.	Deposits from suspension load connected with waning flows or even channel abandonment. Locally affected by pedogenic processes (post-depositional activity) (Miall, 2006).
M1	Mottled dark silty sand or clayey silt, structureless. Admixture of fine grained micaceous sand with irregular, rare scattered pebbles. Base not exposed, irregular erosive concave-down top.	Dominant suspension deposits with limited role of bedload transport via weak currents (Miall, 2006). Floodplain deposits.
M2	Mottled dark sandy silt or clayey silt, structureless. Common root traces and scattered pebbles. Thick bed, broadly tabular. Irregular mostly gradational base.	Floodplain deposits with significant role of pedogenesis (Miall, 2006). Suspension setting in subaqueous floodplain followed by subaerial conditions.

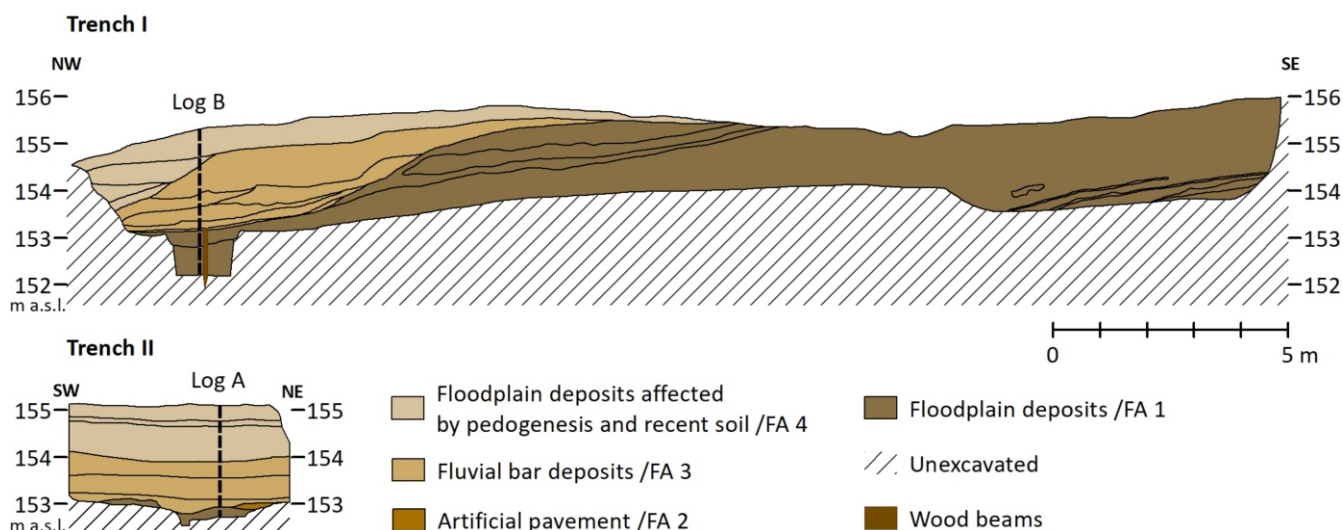


Fig. 2. Simplified sketch of the artificial trenches with positions of the lithological logs

For position of trenches in the area under study see [Figure 1](#)

(sorting) of 2.1 reflects poor sorting. The deposits of FA 1 are covered by the deposits of FA 2 or FA 3.

FA 2 is formed by discoidal or blade-shaped cobbles or even boulders of limestone or sandy limestone (Ga lithofacies), which are layered horizontally i.e. A–B plane parallel to the surface ([Fig. 4B, D](#)). The largest observed clast reached 30 cm in diameter. The clasts are deeply altered due to the effect of subsurface waters so the small size fraction (i.e. pebbles) is preserved only as lenses of whitish sand. There are numerous wood elements. The finds of wood can be divided into several types and the state of wood preservation also varies ([Fig. 4D, E](#)). The first type represents indeterminate pieces of branch, or splinters, rods and beams. Thinner wood lying horizontally are held together by roots growing through the remains of the wood mass. Round and trapezoidal wood fragments with a diameter of ~5 to 12 cm and several dm long were sharpened and driven into the bottom of the fluvial channel (FA 1), vertically or diagonally ([Fig. 4D](#)). These wood elements are overturned. Five massive beams were also found, in an upturned position driven into the underlying bed (i.e. FA 1) to a maximum depth of 0.5 m ([Fig. 4E](#)). During the retrieval and documentation of wooden elements, we also identified triangular wedges filled with gravel ([Fig. 4C](#)). Ceramic shards, animal bones, daub and two millstone fragments were found, randomly scattered among stones and wood fragments, with the highest concentration in the southwestern part of the trench. Deposits of FA 2 were clearly identified only in some parts of the trench studied.

FA 3 is constituted mostly of medium-thick sandy beds of facies Sr, Sl, Sm and Gm with thin interbeds of facies Fl ([Figs. 3A, B and 5A–D](#)). FA 3 was recognised in the middle part of the succession, an erosive broadly concave-down base separating it from FA 1 ([Fig. 5A](#)) or it irregularly interfingering with deposits of FA 2 ([Fig. 4C, E](#)). Lithofacies Sr dominates in the lower portion of FA 3, accompanied here by facies Gm and Fl. Broadly lenticular Gm, Sr and Fl beds with irregular concave-down bases are characteristic. Sandy gravels of lithofacies Gm either directly cover the base of FA 3 ([Fig. 5A, C](#)) or erosively cut underlying sands of lithofacies Sr and are covered by the fine-grained lithofacies Fl. The thickness of Gm beds is highly variable, reaching 20 cm. In some parts of the profile Gm is represented only by row of isolated pebbles. The dominant litho-

facies Sr forms beds about 6 to 20 cm thick ([Fig. 5A–C](#)). A coset of lithofacies Sr can be laterally followed for ~3 m. Facies Fl comprises only cm-scale discontinuous interbeds/interlaminae. Lithofacies Sl dominates in the upper portion of FA 3, accompanied here by facies Sm ([Fig. 5C](#)). Both lithofacies form generally sub-horizontal beds/sheets about 20 cm thick with lateral extents of several metres. A massive/structureless facies Sm passes laterally and vertically into ill-defined planar parallel lamination of facies Sl. A broad fining-upwards trend characterizes FA 3. Palaeocurrent directions measured from cross-lamination and inclined internal surfaces indicate transport towards the south-west (see [Fig. 3](#)).

The deposits of FA 3 are mainly medium- to coarse-grained sands or silty sands with a sand content of 71.4–92.7% ([Fig. 6](#)). The gravel content is very low (0.1–1.0%) similarly to the content of clay (0.4–4.8%). The content of silt varies greatly (6.0–21.8%). The sand content between 70.6 and 81.8% is significantly lower and the fine fractions significantly higher than in the basal parts of the profile (silt: 2.1–8.5%, clay: 0.3–1.1%). The average grain size (mean) of the deposits is between 1.1 and 2.8 Φ (medium/fine sand) and values of 1.5–2.6 of the standard deviation (sorting) reflect poor to very poor sorting.

FA 4 is composed of mottled dark structureless sandy silts and clayey silts with root traces and scattered pebble-sized clasts (facies M 2) and recent soil on the top. They directly overlie the deposits of FA 3 ([Figs. 5D and 8](#)). The deposits of FA 4 have a silt content of 52.6–69.7% ([Fig. 6](#)). The content of sand varies between 7.4 and 36.5% and generally rises in the lower part of the succession. The content of clay also varies (8.9–22.9%), being greater in the upper parts of the FA 4 profile. The average grain size (mean) of the sediments is between 5.3 and 6.8 Φ (medium/fine silt) and values of 1.8 to 2.0 of the standard deviation (sorting) reflect poor to very poor sorting ([Folk and Ward, 1957](#)). The organic content increases towards the top of FA 4. The base is irregular and transitional to the underlying FA 3.

GEOCHEMICAL COMPOSITION

The geochemical data are shown in [Figure 7](#) and [Table 2](#). FA 1 has the highest S values. All other chemical elements de-

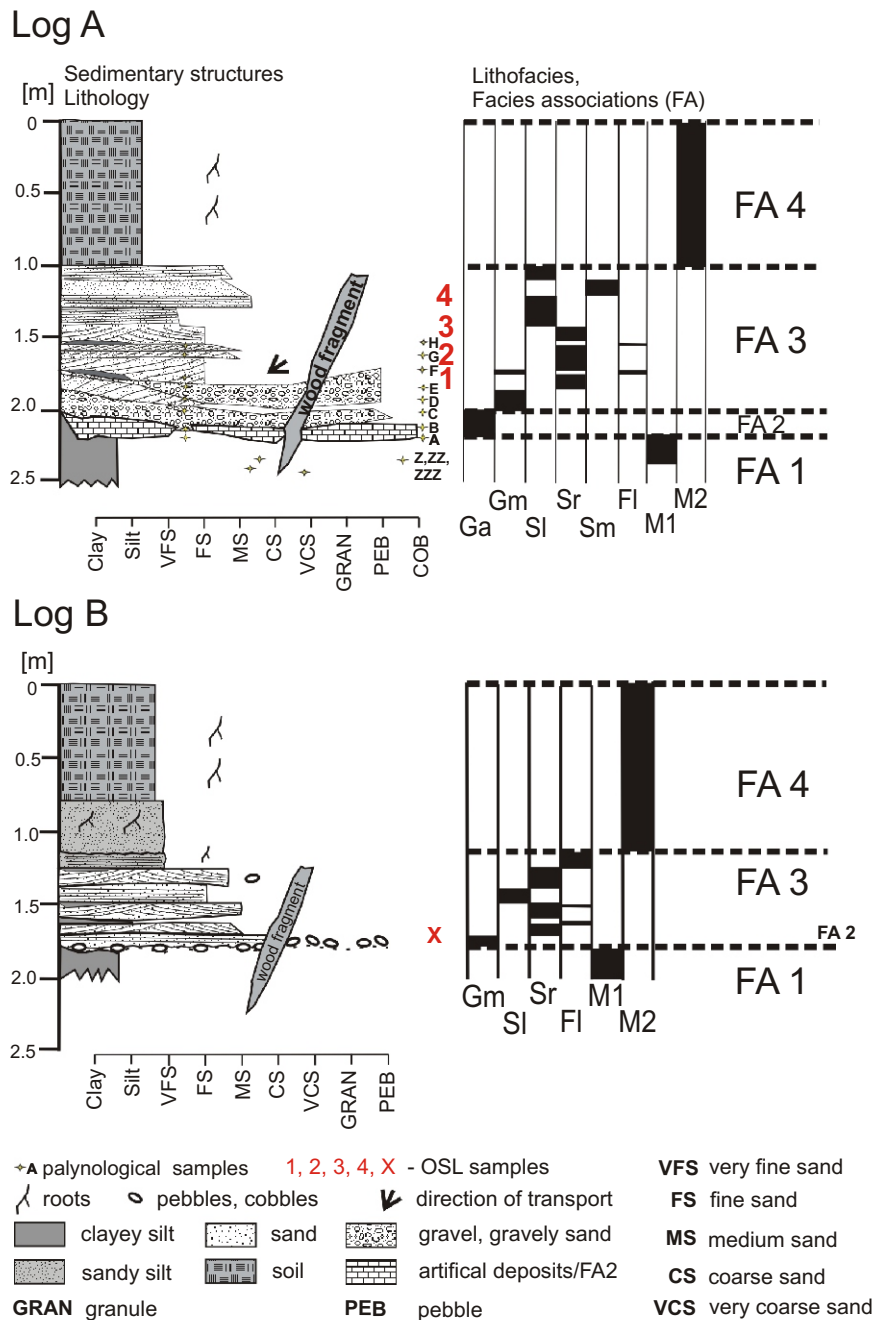


Fig. 3. Schematic lithostratigraphic logs (A and B) of the artificial trenches with distribution of lithofacies, facies associations (FA) and positions of OSL and palynological samples

For positions of logs refer to [Figures 1 and 2](#)

terminated (P, Ca, Ni, Cu, As and Pb) are relatively more abundant in FA 1. The abundance of all these elements decreases in the lower part of the succeeding FA 2, while increasing in its upper part.

In FA 3, values of S are relatively low with three local maxima at depths of 200, 175 and 145 cm. The values of heavy metals are also low and relatively stable except for values of Cu and Ni at the bottom of FA 3. Though P reaches a very low value in the uppermost part of FA 3 (105 cm), values are generally high, and generally show an increasing trend towards the top. In FA 4, S values are stable and low. All values of heavy

metals increase towards the top, with maxima of about 20 cm. The values of Ca also rise and are more or less stable. P reaches high values with local maxima at 95 cm and at the top of the profile.

PALYNOLOGY

The vegetation of the wider surroundings of the floodplain in the early Middle Ages close to the profile studied comprised a mosaic of both forested (mesophile hornbeam woods with lin-

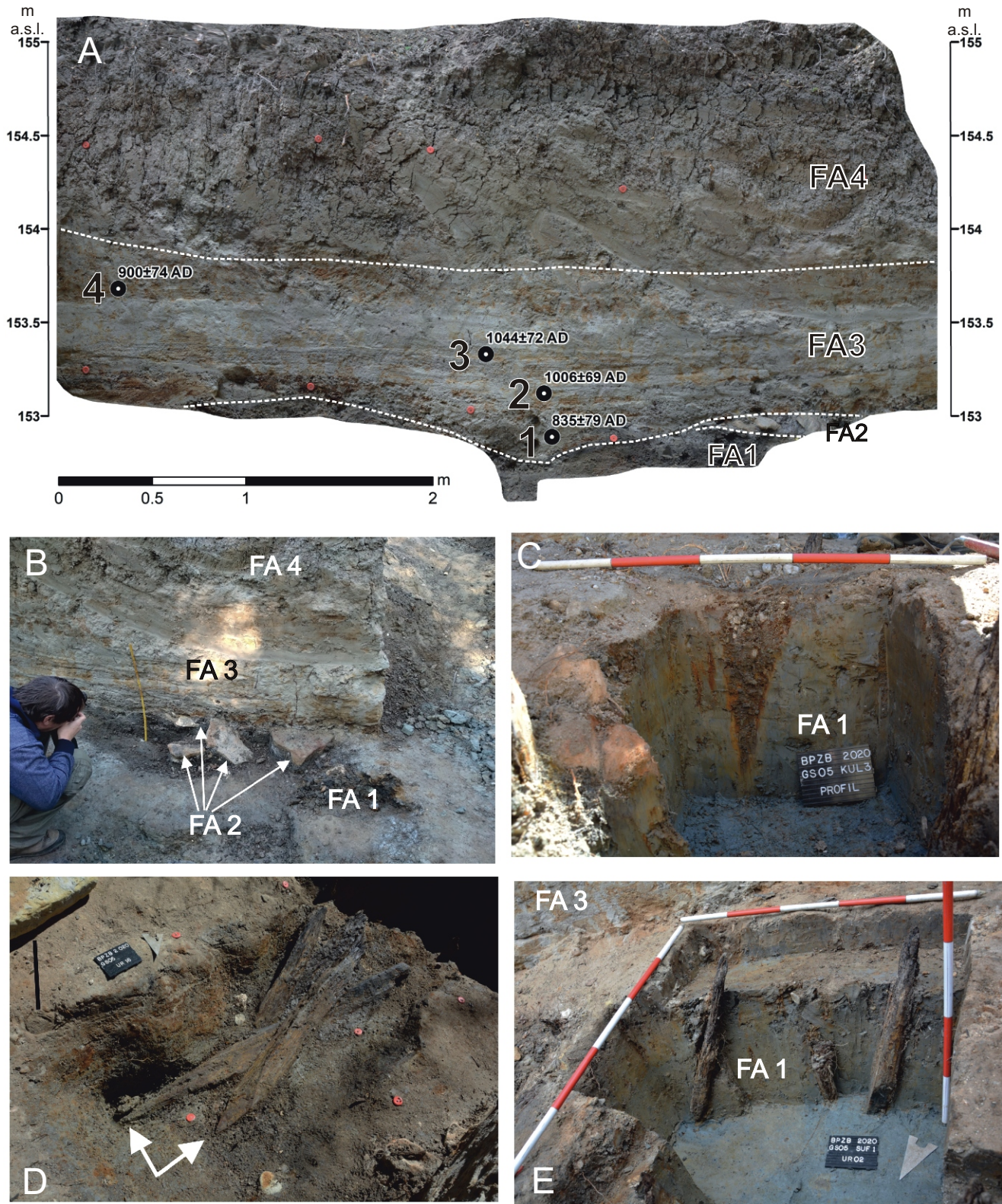


Fig. 4. Photos of exposures in the trench studied

A – photo of the trench wall (where log A was measured) with distribution of facies associations (FAs) and positions and results of OSL samples 1–4; **B** – detailed photo of the trench wall with distribution of the recognized facies associations (FAs); note the position of the cobbles and boulders of FA 2; **C** – deposits of FA1 cut by a triangular wedge filled with gravelly sand; **D** – wood fragments i.e. sharpened stakes in an overturned position (FA2); **E** – vertically and subvertically driven wooden beams (FA 2) in the deposits of FA 1



Fig. 5. Photos of the trench walls studied with selected examples of lithofacies and facies associations

A – erosive contact of deposits of FA 1 (lithofacies M1) and deposits of FA 3 (lithofacies Gm, Sr); **B** – succession of FA 3; **C** – line drawing of the deposits of FA 3; **D** – upper part of deposits of FA 3 with transition to FA 4 deposits; **E** – sedimentary succession studied; notice deposits of FA 2 and FA 4

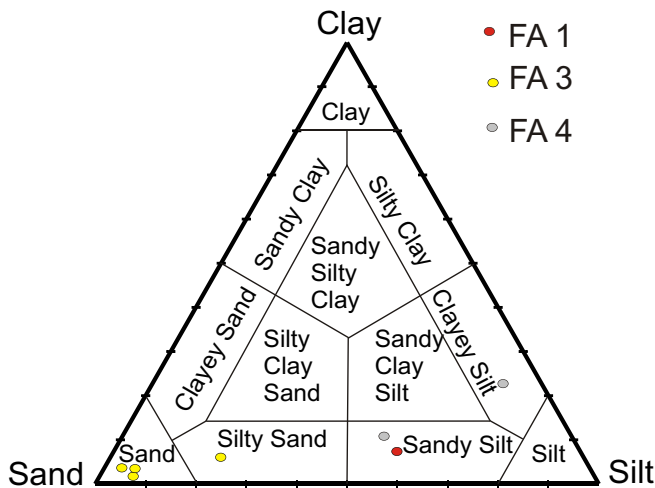


Fig. 6. Results of grain size analysis from Pohansko in a ternary sand-silt-clay diagram (according to Pettijohn et al., 1973, modified)

den trees and alluvial hardwoods and softwood species) and open areas (drier to marshy character) as was shown by earlier palynological and macropalaeobotanical study (e.g., Opravil, 1978, 1983, 2000; Svobodová, 1990; Doláková et al., 2010, 2020). The landscape shows constant human influence (deforestation, grazing, cultivation of crops and the presence of weeds) from the Neolithic (e.g., Svobodová, 1990; Doláková et al., 2010; Dreslerová et al., 2013, 2020; Petřík et al., 2019). 11

samples were analysed palynologically (Table 4). Three samples were taken from clays and sands in the underlayer of wooden stakes (FA 1). Eight samples came from FA 3 and their positions are illustrated in Figures 3 and 8. The higher part of the profile was not suitable for preserving palynomorphs, and therefore lacks a palynological record.

Samples from FA 1 (samples Z–ZZZ) contain mainly Neogene palynomorphs (Fig. 9) (e.g., *Engelhardia*, *Myrica*, *Nyssa*, *Celtis*, *Sciadopitys*, *Cathaya* spores *Leiotriletes wolfii*, *Toroisporis* and marine Dinophytes). The uppermost sample contains a very small number of palynomorphs.

Palynospectra from FA 3 (samples A–H) have a relatively uniform character (except for the uppermost sample H). The vegetation in the area corresponds to that of a typical floodplain close to watercourses. Herbs prevail (65–76%) in all samples, and woody plants make up 24–35% of the association (Table 4). Forested mesophilic habitats were inhabited mainly by oaks (*Quercus*) with a smaller presence of linden (*Tilia*), birch (*Betula*) and an admixture of conifers. Grains of hornbeam (*Carpinus*) are missing in some samples. Marginal scrub is represented by *Prunus*, *Cornus*, *Corylus* and *Sambucus nigra*. Alluvial stands are more frequent: softwood (*Salix* – willow, with less *Fraxinus* – ash) and hardwood (*Alnus* – alder, *Ulmus* – elm). The open areas consisted of dry, slightly wet and wet sites with varying proportions of grasses and changes in the diversity of other herbs. Marsh vegetation connected with watercourses is rich (Cyperaceae, *Typha*, *Potamogeton*, *Caltha*, rare aquatic *Myriophyllum* and *Nuphar*). Human activities are indicated mainly by cereal palynomorphs including *Triticum* (wheat) and *Panicum* (millet) types, as well as by those of *Cucumis sativus* (cucumber), *Apium* (celery) and *Allium* (garlic). *Juglans* (nut-

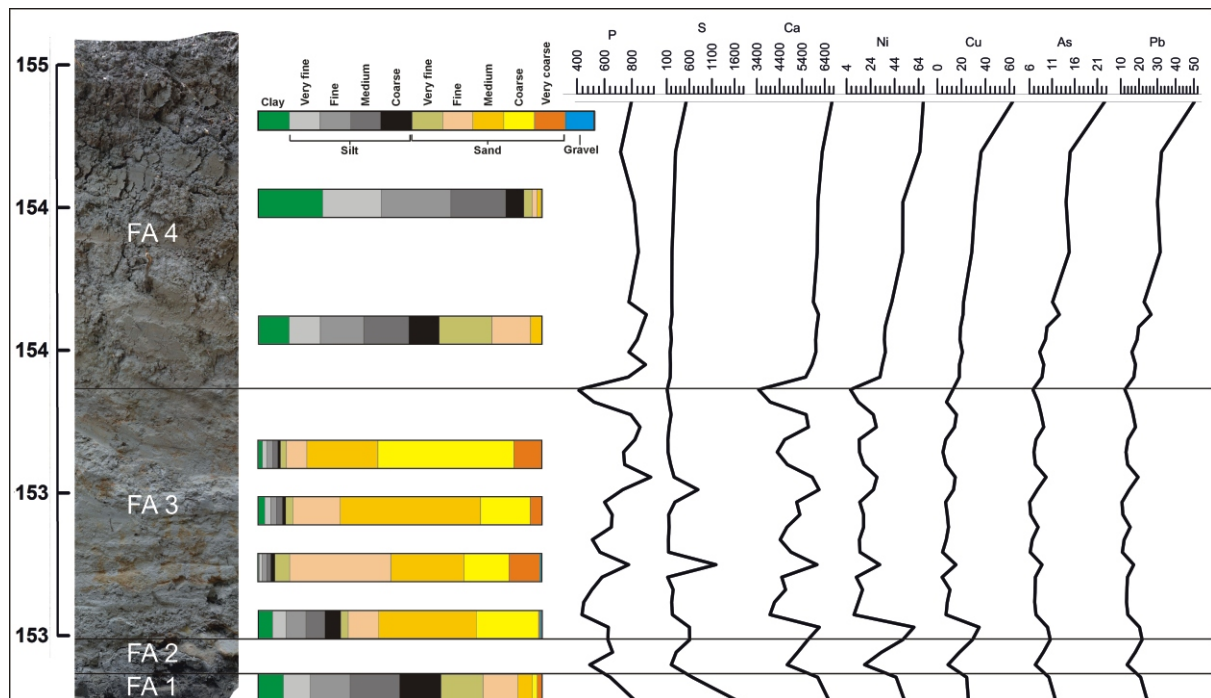


Fig. 7. The results of selected chemical elements and grain-size distributions from trench A in the context of lithofacies

Depth of FAs are slightly shifted from those in Figure 3 because of the different sampling points

Table 2

Results of selected element concentrations and element ratios associated with possibly human activities, grain-size distribution and weathering

Depth [m]	FA	P	S	Ca	Mn	Fe	Ni	Cu	As	Pb	Si/Al	Ti/Al	Rb/Sr
0	4	796	529	6720	387	40500	67.9	62.5	22.6	50.2	3.2	0.06	2.3
0.2	4	717	295	6290	538	46600	65.0	36.3	15.0	32.3	3.2	0.06	3.0
0.4	4	816	258	6100	514	44000	50.9	31.4	14.1	30.1	3.4	0.06	2.6
0.6	4	847	216	6070	761	43100	50.7	28.6	14.8	31.6	3.7	0.06	2.6
0.8	4	778	212	5900	740	30100	41.7	21.7	11.1	22.8	4.3	0.06	1.5
0.85	4	905	217	6130	652	31300	38.8	21.3	12.6	26.6	4.4	0.06	1.5
0.9	4	871	182	6050	685	27400	36.1	19.2	9.8	19.8	4.6	0.06	1.3
0.95	4	839	203	6000	513	26300	35.5	18.7	9.5	19.0	4.6	0.05	1.2
1	4	778	174	6010	507	29100	36.3	20.8	8.2	16.1	4.6	0.06	1.5
1.05	4	899	182	5840	432	29300	33.8	18.3	9.1	18.1	4.9	0.06	1.3
1.1	4	773	178	5560	318	24500	31.8	18.2	8.7	17.2	4.6	0.05	1.2
1.15	4	407	110	3480	102	5170	7.2	ND	6.7	12.3	7.6	0.02	0.6
1.2	3	524	151	3990	142	9400	13.8	7.5	7.9	15.1	6.6	0.03	0.6
1.25	3	791	197	5580	299	21200	26.3	15.8	8.5	16.8	5.4	0.05	1.0
1.3	3	859	152	5680	331	26300	28.8	14.2	9.1	18.1	5.1	0.06	1.1
1.35	3	822	126	4630	266	14700	14.5	6.8	7.4	14.0	6.6	0.03	0.7
1.4	3	739	129	4300	253	12500	14.8	4.5	6.9	12.9	6.8	0.03	0.7
1.45	3	747	186	4750	245	15900	18.4	7.0	7.3	13.8	6.3	0.04	0.8
1.5	3	937	263	5850	307	25800	29.3	14.8	9.6	19.5	5.0	0.05	0.9
1.55	3	733	790	6150	252	18600	26.4	13.4	7.7	14.7	5.0	0.05	0.9
1.6	3	601	281	5160	214	10600	15.0	6.7	6.0	10.7	6.2	0.04	0.6
1.65	3	656	143	5300	236	11800	18.2	8.1	6.2	11.2	6.5	0.04	0.7
1.7	3	650	152	4730	278	15500	18.2	9.2	7.9	15.2	6.1	0.04	0.7
1.75	3	512	138	4430	178	9800	14.7	7.3	6.6	11.9	6.6	0.03	0.7
1.8	3	567	141	4910	313	10700	15.2	4.2	6.1	10.9	7.3	0.04	0.6
1.85	3	776	1190	6060	345	20600	31.6	15.4	8.7	17.1	5.0	0.04	0.9
1.9	3	582	120	4500	328	12000	12.1	3.8	7.3	13.7	7.2	0.04	0.6
1.95	3	508	242	4670	230	11500	17.3	10.4	7.2	13.4	6.0	0.03	0.5
2	3	449	209	4180	208	8150	13.8	8.1	7.1	13.2	6.9	0.03	0.5
2.05	3	436	226	3980	154	7320	10.2	7.1	7.4	13.9	7.0	0.02	0.5
2.1	3	628	602	6160	301	29700	60.1	34.7	9.9	20.3	3.9	0.05	1.6
2.15	3	625	608	5660	289	23900	50.8	29.2	10.6	21.7	4.5	0.05	1.1
2.2	2	659	309	5210	308	19100	33.1	18.4	9.0	18.0	5.2	0.04	0.8
2.25	2	493	201	4740	275	13900	19.0	8.8	7.2	13.5	6.4	0.04	0.8
2.3	2	642	666	6090	320	24200	45.3	24.3	10.3	20.9	4.7	0.05	1.2
2.4	1	837	1730	6630	348	26600	52.8	25.9	11.9	24.8	4.4	0.05	1.4

ND – not detected

cracker) is also recorded in some places in low numbers. Secondary indicators of human presence such as weeds (*Plantago lanceolata*, *Polygonum aviculare*, *Rumex acetosa/acetosella*) and plants demanding an increased nitrogen content (Chenopodiaceae including *Chenopodium bonus-henricus*, *Artemisia*,

Asteraceae/Liguliflorae, *Galium*) are obvious. The highest sample (H) of the profile (Figs. 8, 9 and Table 3) contains the fewest indicators of human activities.

Observing the palynospectra of FA 3 in detail, changes in quantitative representation of individual plants can be observed

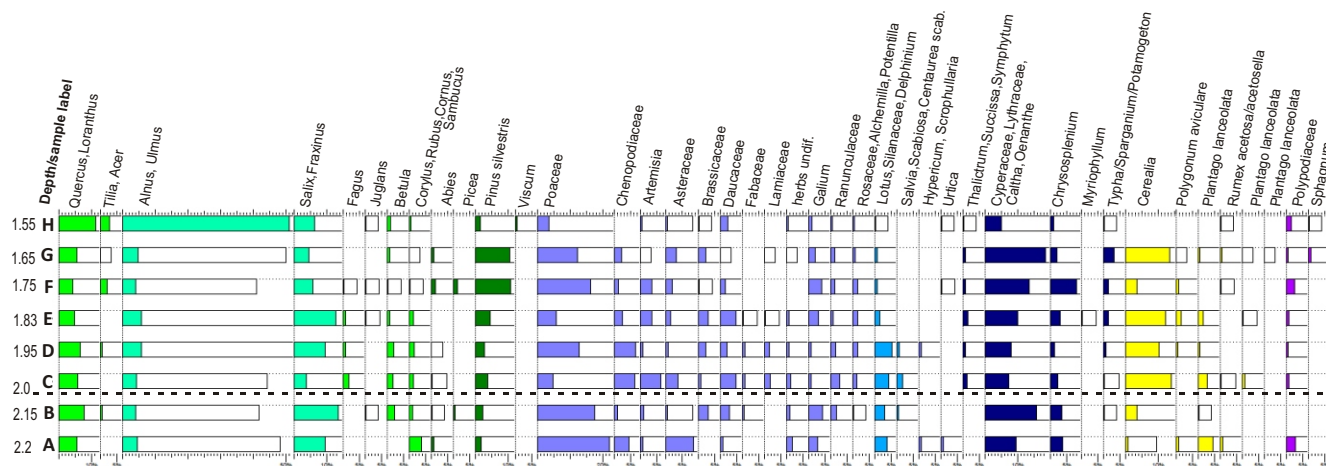


Fig. 8. Pollen diagram of the profile studied (FA 3)

Individual plant groups colour-coded: trees and shrubs – green, herbs – blue, anthropogenic – yellow, ferns – violet, black hatched line – samples from artificial pavement sublayer

in the succession (see Fig. 8). The lowermost samples (A, B) have the highest proportion of grasses and low amounts of human indicators. A noticeable change is connected with the samples in the middle of the FA 3 succession (C, D, E, see Fig. 8). A decrease in softwood alluvial forests and in grasses with an increase in the variety of herbs and the highest representation of cereals and nitrophilous indicators (*Chenopodiaceae*, *Artemisia*) are observed here, as is an increase in the proportion of herbs of dry habitats (*Centaurea*, *Delphinium*, *Lotus*, *Salvia* and other) accompanied by a decrease in swamp signals (*Cyperaceae*, *Lythraceae*).

The diversity of the herbal spectrum (especially dry habitats) decreases in the upper part of the FA 3 succession (samples F, G). An increase in the content of moisture-loving herbs and floodplain trees as well as an increase in the content of *Pinus* was observed. The finding of a *Trichiuris* (roundworm) egg together with more cereals (in the sample G) indicate human activity.

A relatively large change can be seen in the highest palynological sample (sample H). Arboreal pollen of a hardwood floodplain forest prevails in the association (especially *Alnus* – 75%). However, alder produces pollen in catkins, and therefore these pollen contents in the sediment can lead to overestimates of overall tree frequency. The highest representation of oak pollen can also be observed here. There is absence of cereals and few other anthropogenic indicators.

GEOCHRONOLOGY OF THE DEPOSITS

Ceramic shards, specifically fragments of the edges and bulges of Mikulčice ceramics assigned to the middle hillfort period of Great Moravian period, were found in FA 2. This ceramic type is allocated to the second half of the 9th and the first half of the 10th century at Pohansko as well as at a nearby archaeological site of Valy u Mikulčic (Macháček, 2001; Mazuch, 2013).

The felling of wood D18, found in an upturned position with its point pointing into pillar pit 2 (Fig. 4D, E), is dendrochronologically dated to 894 CE.

The position of OSL samples 1–4 is shown in Figures 3A and 4A and the position of sample X is visible in Figure 3B. Ex-

cept for one sample (sample 4), the date of which is inconsistent with the stratigraphy, the OSL dating indicates the accumulation of FA 3 in the period between 9th and 11th centuries (Table 3).

DISCUSSION

The results of multidisciplinary research in the Dyje River floodplain near Early Mediaeval archaeological site Pohansko illustrate primary shifts in the Late Holocene river dynamics, most specifically in the Mediaeval period. The study site provided insights into the impact of human influences on the fluvial sedimentary deposits through various local/direct and distal/indirect agents. Effective time control of the deposits enabled connection of these signals with processes in the river catchment.

One of the consequences of climatic warming at the Pleistocene-Holocene transition was a change of the fluvial style of rivers in Europe and North America from braided depositional styles to meandering or anastomosing (Gibbart and Lewin, 2002; Bábek et al., 2018). The strong predominance of overbank facies (FA 1 and FA 4) over channel infill facies (FA 3) seems to signalize an anastomosing fluvial style of the Dyje River. Triggered channel avulsion might be explained by processes in the floodplain (e.g., variations in vegetation cover, intensity of agricultural activities or and further anthropogenic interventions). Climatically conditioned phases of increased fluvial activity have been documented in many central European large river systems and dated mostly to the 10th century (Kalicki, 2006).

OLDER OVERBANK DEPOSITS

The monotonous deposits of FA 1 reflect dominant deposition from suspension with only limited bedload transport via weak currents and these are interpreted as overbank deposits. These deposits probably drape underlying Neogene (Pannonian) lagoonal to open lake deposits of the Vienna Basin (Nehyba et al., 2020) which partly served as a source of the FA

Table 3

Comprehensive table of determined pollen and spores taxa and their sums in individual samples

Sample number	H	G	F	E	D	C	B	A	X	XX	XXX
Depth [cm]	155	165	175	183	195	200	205	220	230	240	250
Arboreal pollen (AP)											
<i>Abies</i>		3	3		1	1	1	1			
<i>Acer</i>	1										
<i>Alnus</i>	115	8	7	10	13	8	10	3	2		
<i>Betula</i>	3	3	1	2	6	4	6		1		
<i>Cornus</i>				2	1		2	1			
<i>Corylus</i>				1	2	3			1		
<i>Fagus</i>			1	2	3	4					
<i>Fraxinus</i>	2	1	2	2	6	1	7	3			
<i>Juglans</i>	1		1	1			1				
<i>Loranthus</i>						1					
<i>Picea</i>			3				2				
<i>Pinus silvestris</i>	4	30	24	10	8	8	6	2	1		
<i>Quercus</i>	27	16	10	11	18	11	19	6	2		
<i>Rubus</i> t., <i>Prunus</i>	2	1			2			2			
<i>Salix</i>	13	12	11	26	20	7	26	7	2		
<i>Sambucus nigra</i>			1				1	1			
<i>Tilia</i>	6	1	6		2		2				
<i>Ulmus</i>	5	6	4	3	3	1		2			
<i>Viscum</i>	2										
sum of AP	181	81	74	70	85	49	83	28	9		
Nonarboreal pollen (NAP)											
<i>Artemisia</i>	2	1	8	8	3	13	3	1	2		
Asteraceae Liguliflorae		6	1	1	1	5		4	1		
Astraceae Tubiflorae	2	4	4	3	2	3	2	5	1		
Brassicaceae			1	7	3						
t. <i>Barbarea</i>	1	7			4	2	6				
t. <i>Cardamine</i>							2				
<i>Centaurea</i> sp.				1							
<i>Centaurea jacea</i>		4	1		2	4					
<i>Centaurea scabiosa</i>					1	1	1				
<i>Cerealía</i>		38	7	26	28	26	9		2		
<i>Panicum</i> type			1	1		3		1			
<i>Cerinte</i>	1										
<i>Cucumis sativus</i>					1						
<i>Cuscuta</i>						2					
Cyperaceae	12	51	25	21	21	13	37	9			
Daucaceae	4	1	2	9	4	4	7				
<i>Daucus</i> t.			2		2	4					
<i>Oeanthe</i>							1				
<i>Apium</i>	2			2				1			
<i>Peucedanum palustris</i>						2					
<i>Chaerophyllum bulbosum</i>				2	1						
<i>Euphorbia</i>		1					1				
<i>Euphrasia</i>	1							1			
Fabaceae				1	2	2	2				
<i>Dorycnium</i>					2						
<i>Lotus</i> t.		1		1	4	2		1			
<i>Trifolium/Lathyrus</i>					1						
<i>Galium</i>	3	6	9	7	3	2	11	3			

Tab. 3 cont.

Sample number	H	G	F	E	D	C	B	A	X	XX	XXX
Depth [cm]	155	165	175	183	195	200	205	220	230	240	250
<i>Humulus/Cannabis</i>		1		1		2					
<i>Hypericum/Scrophularia</i>					3			1			
Chenopodiaceae		6	3	6	15	11	3	3	2		
<i>Chenopodium bonus-henricus</i>		1			3	2		2			
<i>Chrysosplenium</i>	3	6	18	7	4	5	9	4	1		
Lamiaceae		1		1	3	4					
<i>Teucrium</i>					2						
<i>Salvia</i>					1	3	1				
Liliaceae <i>Scilla t./Allium</i>				1	3	1	1				
<i>Malva neglecta</i>		1									
<i>Myriophyllum</i>				1							
<i>Oxalis acetosella</i>								1			
<i>Papaver rhoeas</i>							1				
<i>Plantago lanceolata</i>		1	2	4	2			1			
Poaceae	9	35	36	13	35	10	42	23	6		
<i>Polygonum aviculare</i>		2		4	2	6	1	5			
Ranunculaceae	2	4	3	2	3	4	5		1		
<i>Anemone/Pulsatilla</i>					2	2					
<i>Caltha</i>		1	5	1	1						
<i>Delphinium</i>	1	2	2	2	6	5	8	2			
Rosaceae	2	1	1		4	1	1		1		
<i>Alchemilla</i>		2	3	3		1					
<i>Potentilla</i>				1	1	1					
<i>Sanguisorba officinale</i>									1		
<i>Rumex acetosa/acetosella</i>	1	2	1			1		1			
Silenaceae				1	3	2		1			
<i>Typha/Sparganium/Potamogeton</i>	1	10	4	4	2	1	1				
<i>Nuphar</i>	1				1						
<i>Succisa</i>						1					
Lythraceae						2		1			
<i>Scabiosa</i>					1						
<i>Symphytum</i>	1	1	1	1	2						
<i>Urtica</i>	1		1					1			
<i>Thalictrum/Illecebrum</i>		2	1	2		2					
sum of NAP	51	200	142	145	186	155	155	72	18		
suma AP	181	81	74	70	85	49	83	28	9		
sum of AP + NAP	232	281	217	215	271	204	238	100	rare pollen		
AP: NAP v%	78:22	28:72	34:66	32:68	31:69	24:76	35:65	28:72			
Sporophyta											
Polypodiaceae smooth	4	2	6	2	2	2		3	1		
<i>Sphagnum</i>	1	3							1		
<i>Pteridium typ</i>	1										
<i>Riccia</i>		3									
Fungi											
Algae											
<i>Botryococcus</i>		x	xxx	x	x	x	xxx	x			
<i>Glomus</i>		x	x	x	xx		xxx	x			
<i>Rivularia</i>	xx	x	x	x	x	x					
<i>Trichiuris egg</i>		1									
Neogene pollen /reposition	1		5	2	5	4			4	35	20

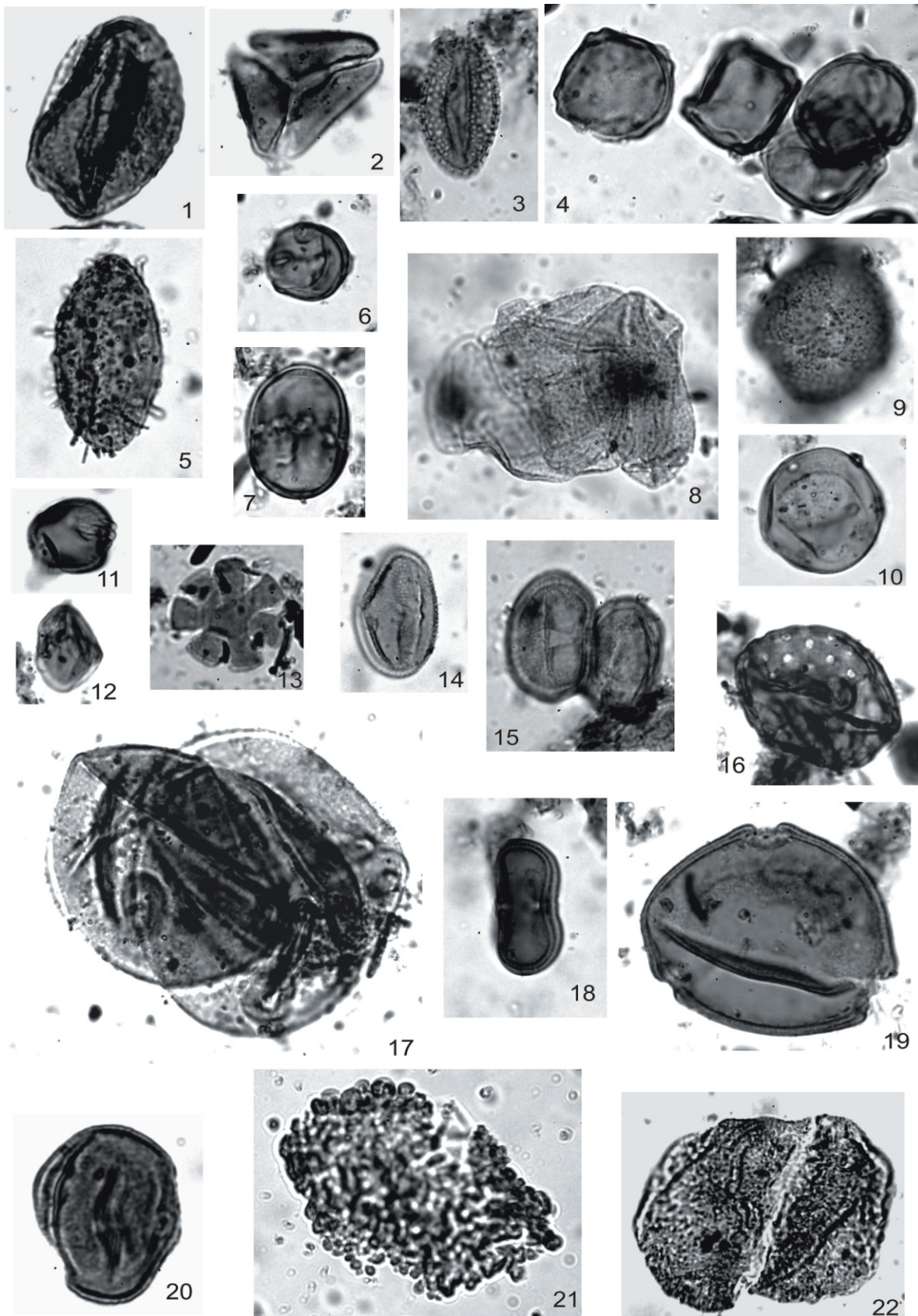


Fig. 9. Photos of typical pollen from the deposits studied

1 – *Quercus* – H; 2 – *Loranthus europaeus* – C; 3 – *Salix* – H; 4 – clump of *Alnus* – H; 5 – *Nuphar* – H; 6 – *Myriophyllum* – E; 7 – *Symphytum* – E; 8 – clump of *Cyperaceae* – G; 9 – *Caltha* type – H; 10 – *Humulus/Cannabis* – E; 11 – *Potentilla* – C; 12 – *Prunus* – D; 13 – *Salvia* – C; 14 – *Hypericum/Scrophularia* – D; 15 – *Polygonum aviculare* – C; 16 – *Chenopodium bonus-henricus* – D; 17 – clump of *Cerealia-Triticum* type – C; 18 – *Daucus carota* type – D; 19 – *Cucumis sativus* – D, Neogene pollen; 20 – *Nyssa* – XX; 21 – *Sciadopitys* – XX; 22 – *Cathaya* – X

1 deposits, as corroborated by palynology (see chapter Geochronology of the deposits, Table 4). *In situ* Neogene (Pannonian) palynological associations have been observed from the lower part of earlier-studied boreholes at Pohansko. Redeposited Neogene palynomorphs have previously been observed in Holocene deposits (Macháček et al., 2007; Doláková and Kováčová, 2008; Doláková et al., 2010).

The beginning of sedimentation of the older overbank deposits at Pohansko as well as at the nearby archaeological site of Mikulčice is estimated to be in the Late Holocene, ~4000–3000 BP (Opravil, 1983; Havlíček, 2001, 2004; Břízová and Havlíček, 2002; Havlíček and Smolíková, 2002). According to Opravil (1999) the first erosion and accumulation of such overbank sediments was associated with the ploughing of fields on the upper reaches of rivers during the Bronze Age in the region. The same trend is generally visible in Central Europe fluvial archives with the first erosion period dated to the Late Bronze Age and Iron Age (Dreibrodt et al., 2010). Based on dating of the overlying deposits of FA 2 and FA 3 and the sedimentological characteristics of FA 1, we infer that the FA 1 deposits may be analogous to the older overbank deposits noted above. The overbank deposits have increased concentrations of P and S as well as of heavy metals, which could be associated with either natural processes or human activities (e.g., Schlezinger and Howes, 2000; Holliday and Gartner, 2007). Macroscopically, the FA 1 deposits contained much organic matter, which may be reflected in higher contents of P and S as well as of heavy metals, which may be bound to organics (Kwiatkowska-Malina, 2018). Moreover, before the 9th century, the human activities in the area are very rarely detected (Dostál, 1968). Therefore, we infer that the higher concentration of these elements does not correspond to signals of human activity in the catchment.

of a wooden structure. We interpret the round and trapezoidal wood elements as stakes. Some stakes were driven vertically or diagonally and were part of structures of unknown function, perhaps a system for catching fish. The triangular wedges filled with gravel are interpreted as evidence of stakes, which were pulled out in the past, either intentionally by humans or due to the action of ice and water level fluctuations. Massive and large wooden beams in vertical or isolated positions were interpreted as remnants of a bridge (Nehyba et al., 2020). A similar wooden bridge construction was documented in the nearby Mikulčice Great Moravian centre (~15 km NE of the Pohansko site) (Poláček and Hladík, 2014).

A piece of construction wood was dated to year 894 CE. This age is supported by a combination of radiocarbon dating and dendrochronology of another wood fragment (D17) of which the most probable time of felling was estimated at between 841 and 842 CE (Nehyba et al., 2020). A numerical age of OSL sample 1 from the overlying FA 3 was calculated to the interval from 756 to 914 CE (Table 3). We therefore can expect the start of FA 2 accumulation between 894 and 914 CE. The construction of a pavement and wooden structure may correlate with the Early Mediaeval activities at Pohansko dated to the end of 9th and/or the beginning of 10th centuries CE when Pohansko became the Great Moravian centre (Macháček et al., 2021).

The deposits of FA 2 show clear and rich evidence of anthropogenic activities which directly affected the depositional elements within the fluvial channel. The concentrations of chemical elements which can be referred to human activities (e.g., P or heavy metals) are low in the basal part of FA 2 which reflect a signal of natural palaeochannel deposits. However, the signal increases in the upper part, probably reflecting the onset of constructional activities at the site.

Table 4

Results of OSL dating of the samples

Sample	OSL age	Resulted dating (AD)
X	1.183 (72) ka	767 (72)
1	1.115 (79) ka	835 (79)
2	0.944 (69) ka	1006 (69)
3	0.906 (72) ka	1044 (72)
4	1.050 (74) ka	900 (74)

For position of the samples refer to Figures 3 A, B and 4A

ARTIFICIAL PAVEMENT AND WOOD CONSTRUCTIONS

FA 2 is interpreted as an artificial pavement with wooden constructions built on the bottom of a fluvial palaeochannel which eroded older overbank deposits (FA 1) and the accumulation of which consequently continued as FA 3. The fluvial palaeochannel itself served probably as a part of the defence system of the Pohansko stronghold, and so there might have been demand for stabilisation of the river course. We interpret the cobbles and boulders as a human attempt to stabilize the bottom of the fluvial channel. The indeterminate branch fragments can mostly be considered as structural elements of unknown purpose. We also consider splinters that could have been driven into the bottom of palaeochannel and serve as part

FLUVIAL CHANNEL DEPOSITS

Deposits of FA 3 are interpreted as fluvial channel deposits/ i.e. a side or point bar. Lithofacies Gm was deposited in the middle to upper part of the lower flow regime and interpreted as an incipient channel gravel bar and channel lag (Miall, 2006).

Thin interlaminae of lithofacies F1 are interpreted as deposits from suspension load connected with waning flows or even channel abandonment (Miall, 2006). Most deposition occurred from suspension settling with only limited bedload transport via weak currents. Beds of facies F1 represent erosional relics connected with erosive flow after a stillstand event.

Beds of lithofacies S1 are interpreted as tractional deposits connected with the upper flow regime, higher fluvial discharge and the upper parts of the fluvial dune/bar. The prevalent lithofacies Sr was formed by migration of ripple bedforms in flowing shallow water and a lower flow aggradational regime (Best, 1996). The rippled beds can be regarded as indications of the marginal parts of the channel, and/or deposition in areas of slack or sluggish water on the bar or along its peripheral parts.

Small sets of Sr cross-lamination indicate very shallow but faster currents (Best, 1996). On the other hand, lithofacies Sr points to a flow with limited bedload concentration (Sumner et al., 2008). Rippled beds are often formed by flows with sediment concentrations of 0.01–0.2 g/l (Simons et al., 1965). These are conditions typical of lowland rivers in temperate climates, where washload concentration is in the range of 0.02–0.4 g/l (Mulder and Syvitski, 1995; Skolasińska and Nowak, 2018; Zieliński and Widera 2020). Such conditions can be attributed to periods of inter-flood discharge, especially in shoal

zones. Missing climbing ripples, which are associated with final phases of waning floods, reveal a relatively stable condition of deposition and relatively limited sediment load. However, the interbed of lithofacies Gm and lithofacies FI points to a highly variable fluvial discharge. Thus, a high frequency of Sr lithofacies together with the absence of fluvial dunes is additional evidence that the lower section of FA 3 deposits were formed by flows with limited load (Simons et al., 1965).

The typical interpretation of lithofacies SI is formation under upper plane bed conditions and in connection with fluvial bar tops (Miall, 2006). However, Allen and Leeder (1980) found that a significant increase of bedload concentration resulted in bedform disappearance and the inception of a plane bed configuration (Zieliński and Widera, 2020). Similarly, the Sm lithofacies records rapid deposition of sand predominantly from suspension in a decelerating flow where the rate of deposition was too rapid to allow primary structures to form (Zieliński and Widera, 2020). Both lithofacies SI and Sm occurred in the upper part of FA 3. Therefore, an increased sediment load of the flows is inferred for this part of the FA 3 succession by contrast with its lower portion. The generally fining-upwards trend of FA 3 points to an active successive filling of the palaeochannel accompanied by migration of the channel axis/ thalweg.

Approximately 40 cm of fluvial sands of FA 3 was dated from the 9th to 11th centuries CE. The inconsistent age of OSL sample 4 might have been caused by incomplete resetting of the signal of some grains, as suggested by Wallinga (2008). We can suppose relatively significant sediment supply into the fluvial channel during a hypothetical 200 years. Looking at the river geomorphology and sedimentary record, it may be suggested that the channel deposits studied represents one channel of an anastomosing Dyje River. An anastomosing style reflects increased bedload and flow as occurs during flood events (Makaske, 2001). The pace and nature of the filling of fluvial channels depend on the flood regime (sediment supply) as well as on local controls (distance from the main channel, vegetation, diversion angle, water table level) (Gautier et al., 2007; Constantine et al., 2010; Toonen et al., 2012; Dépret et al., 2017). The facies analysis suggests an upwards increase in sediment load for this part of the succession. The increase in sediment delivery during the period probably reflects some increase in erosion within the catchment area (i.e. more distant to the site). The reason for this may have been either climatic (more extreme climatic conditions) or human activity (such as deforestation). However, the fluvial channel was relatively stable in the area without any clear signal of erosive scours connected with large floods or channel abandonment (Brooks, 2003). FA 3 did not reveal direct evidence of human activities. Values of heavy metals correlate with grain size changes (see Al/Si and Ti/Al) and with organic content (see S), but in some parts may reflect past human activities. Increased values of Cu and Ni are especially noticeable at the bottom of FA 3, which may be connected with human activities at the end of the 9th century CE and/or at the beginning of 10th century CE when Pohansko was an Early Mediaeval centre (Macháček, 2005; Dresler, 2016). In general, FA 3 has generally similar attributes to the floodplain deposits of unit 3 in Trench 1 in the NE suburb of Pohansko, which were interpreted as channel or distal deposits (Petřík et al., 2019). However, the age indicated in this paper (9th–11th century CE) remains older compared to unit 3 of the SE suburb (dated to the 15th century). Changes in human activity are also evident from the pollen diagram (Fig. 9). The greatest human impact was observed in the middle part of FA 3 with the highest amount of cereals and nitrophilous indicators (Chenopodiaceae, *Artemisia*) indicating agricultural activities in the surrounding area, consistent with previous studies

(e.g., Doláková and Kováčová, 2007). In the highest part, cereals completely disappeared which may reflect reduction in the intensity of agriculture connected with abandonment of the stronghold in the first part of the 10th century CE (Macháček, 2005).

YOUNGER OVERBANK DEPOSITS

Deposits of FA 4 are interpreted as overbank sediments deposited after the 11th century CE, with significant signs of pedogenesis. The sharp and abrupt transition between FA 3 and FA 4 as well as the change of grain-size distribution (from sands of FA 3 into silty muds of FA 4) is probably connected with channel abandonment due to avulsion upstream. This means that fluvial system underwent a significant change in the area under study. Channel deposition was followed by a floodplain deposition as the river course was transformed. The root traces in the upper part of FA 4 suggest prolonged subaerial exposure following suspension settling on a floodplain, which led to the development of Fluvisol (IUSS Working Group WRB, 2014). The occurrence of Fluvisol is typical of extensive floodplain areas and has already been described and studied from the area and its surroundings (Adameková et al., 2022).

FA 4 is very similar to unit 4 of Trench 1 (log B) in the NE suburb of Pohansko in terms of lithology (silt, sandy silt interpreted as overbank deposits) and thickness (Petřík et al., 2019). The time of deposition of unit 4 is estimated at the 15th to 20th centuries CE according to dating which preceded the period of bypass and non-deposition within the Dyje floodplain from 11th to 15th centuries CE (Petřík et al., 2019). We therefore infer that the overbank deposits under study started to accumulate from the 15th century at the earliest. Kadlec et al. (2009) reported aggradation of the neighbouring Morava River floodplain since the 13th century. Although the depositional rates of these two rivers are generally in concordance (Dyje: 0.17–0.2 cm/yr and Morava: 0.2 cm/yr) the temporal and spatial variation in sedimentation on these floodplains may have been connected with the different sizes of the individual river basins, variations in fluvial channel dimensions, sediment load, and the history and extent of Middle age colonization. Increasing aggradation of fluvial sediments in the Post-Mediaeval and Modern periods was in general recorded all across Central Europe (e.g., Starkel et al., 2006; Dreibrodt et al., 2010). FA 4 is clearly human-impacted as reflected by increasing trends of heavy metals and phosphorus. Similar increased concentrations of heavy metals were also documented in the overbank deposits of unit 4 (Petřík et al., 2019) and were also reported for the sediments of Morava River dated to the 20th century CE (Bábek et al., 2008; Grygar et al., 2011). The highest values in the upper part of FA 4 are comparable to recent soils captured in trench R 18 (Adameková et al., 2022).

CONCLUSIONS

Multidisciplinary examination of Dyje River sediments deposited in close proximity to the Early Medieval fortified site of Pohansko allowed identification of its depositional environment, the reconstruction of processes in the river catchment and provided information on human influences in the catchment, mainly during the Medieval period.

The lowermost part of the succession studied was interpreted as Late Holocene overbank deposits accumulated before the 9th century CE. Palynology corroborated the important

role of Neogene (Pannonian) deposits of the Vienna Basin in their source area. These deposits are overlain by a tabular to broadly wedge-shaped bed of mostly rippled and laminated sands deposited above the erosive base covered by a pebble lag. This most prominent part of the succession was interpreted as fluvial channel deposits accumulated in the period between the 9th and 11th centuries CE. Flat limestone cobbles and boulders locally interfingered with these fluvial channel sands and covered the base of the fluvial channel. They were interpreted as an artificial pavement. Moreover, numerous wood elements as massive stakes and beams were recognized in upturned positions driven into the basal overbank deposits. These wood fragments were interpreted as an anthropogenic construction, serving as a bridge, an unknown fishing system or wooden structure spanning the years 894 to 914 CE. Both artificial constructions are associated with the period of greatest human ac-

tivity on the directly adjacent Early Mediaeval fortified site of Pohansko. Palynological studies corroborate the highest intensity of agriculture in the river catchment at this time, with its reduction upwards in the succession. In the lower part of the palaeochannel sands, elemental concentrations associated with human activities also increased.

The uppermost part of the succession studied is represented by younger overbank deposits with a recent Fluvisol at the top, the accumulation of which started after the 11th century CE.

Acknowledgements. The study was supported by the project grant GAČR GA20-18929S Fortification Systems of the Great Moravian Centre Pohansko near Břeclav. We thank M. Wardas-Lasoň and two anonymous reviewers for their helpful comments.

REFERENCES

- Adameková, K., Petřík, J., Dlapa, P., Přišťáková, M., Nehyba, S., Dresler, P., Hrabovský, A., 2022. Soil development on the floodplain of the river Thaya in the foreland of the Pohansko stronghold near Břeclav (in Czech). *Geological Research in Moravia and Silesia*, **29**: 78–85. <https://doi.org/10.5817/GVMS2022-33071>
- Allen, J.R.L., Leeder, M.R., 1980. Criteria for the instability of upper-stage plane beds. *Sedimentology*, **27**: 209–217.
- Bábek, O., Hilscherová, K., Nehyba, S., Zeman, J., Famera, M., Franců, J., Holoubek, I., Machát, J., Klánová, J., 2008. Continuation history of suspended river sediments accumulated in oxbow lakes over the last 25 years. *Journal of Soils and Sediments*, **8**: 165–176.
- Bábek, O., Sedláček, J., Novák, A., Létal, A., 2018. Electrical resistivity imaging of anastomosing river subsurface stratigraphy and possible controls of fluvial style change in a graben-like basin, Czech Republic. *Geomorphology*, **317**: 139–156. <https://doi.org/10.1016/j.geomorph.2018.05.012>
- Best, J.L., 1996. The fluid dynamics of small-scale alluvial bedforms. In: *Advances in Fluvial Dynamics and Stratigraphy* (eds. P.A. Carling and M.R. Dawson): 67–125. Wiley, Chichester.
- Beug, H.J., 2004. Leitfaden der Pollenbestimmung für Mitteleuropa und angrenzende Gebiete. Verlag Dr. Friedrich Pfeil, München.
- Bintliff, J., Degryse, P., 2022. A review of soil geochemistry in archaeology. *Journal of Archaeological Science: Reports*, **43**: 103419. <https://doi.org/10.1016/j.jasrep.2022.103419>
- Brooks, G., 2003. Holocene lateral channel migration and incision of the Red River, Manitoba, Canada. *Geomorphology*, **54**: 197–215. [https://doi.org/10.1016/S0169-555X\(02\)00356-2](https://doi.org/10.1016/S0169-555X(02)00356-2)
- Brown, A., Toms, P., Carey, C., Rhodes, E., 2013. Geomorphology of the Anthropocene: time-transgressive discontinuities of human-induced alluviation. *Anthropocene*, **1**: 3–13. <https://doi.org/10.1016/j.ancene.2013.06.002>
- Brown, A.G., Lespez, L., Sear, D.A., Macaire, J.J., Houben, P., Klimek, K., Brazier, R.E., Van Oost, K., Pears, B., 2018. Natural vs anthropogenic streams in Europe: history, ecology and implications for restoration. *Earth-Science Reviews*, **180**: 185–205. <https://doi.org/10.1016/j.earscirev.2018.02.001>
- Břizová, E., Havlíček, P., 2002. Some remarks to the pollen analysis of Quaternary deposits from Mikulčice in southern Moravia (in Czech). *Zprávy o Geologických Výzkumech v r 2001*, **1**: 124–126.
- Candel, J.H.J., Kleinhans, M.G., Makaske, B., Hoek, W.Z., Quik, C., Wallinga, J., 2018. Late Holocene channel pattern change from laterally stable to meandering caused by climate and land use changes. *Earth Surface Dynamics*, **6**: 723–741. <https://doi.org/10.5194/esurf-2018-31>
- Colombera, L., Mountney, N.P., 2019. The lithofacies organization of fluvial channel deposits: a meta-analysis of modern rivers. *Sedimentary Geology*, **383**: 16–40. <https://doi.org/10.16/j.sedgeo.2019.01.011>
- Constantine, J.A., Dunne, T., PiéGay, H., Mathias Kondolf, G., 2010. Controls on the alluviation of oxbow lakes by bed-material load along the Sacramento River, California. *Sedimentology*, **57**: 389–407. <https://doi.org/10.1111/j.1365-3091.2009.01084.x>
- Cook, E.R., Kairiukstis, L.A., 1990. *Methods of Dendrochronology. Applications in the Environmental Sciences*. International Institute for Applied Systems Analysis. Kluwer Academic Publishers, Dordrecht.
- Dépret, T., Riquier, J., Piégay, H., 2017. Evolution of abandoned channels: Insights on controlling factors in a multi-pressure river system. *Geomorphology*, **294**: 99–118. <https://doi.org/10.1016/j.geomorph.2017.01.036>
- Doláková, N., Kováčová, M., 2007. Pannonian vegetation from the Northern part of Vienna basin. *Sborník Národního muzea v Praze*, **64**: 163–171.
- Doláková, N., Roszková, A., Přichystal, A., 2010. Palynology and natural environment in the Pannonian to Holocene sediments of the Early Mediaeval centre Pohansko near Břeclav (Czech Republic). *Journal of Archaeological Science*, **37**: 2538–2550. <http://dx.doi.org/10.1016/j.jas.2010.05.014>
- Doláková, N., Kočár, P., Dresler, P., Dreslerová, G., Kočárová, R., Ivanov, M., Nehyba, S., 2020. Development of interaction of the environment and the subsistence strategy of early medieval society: Pohansko near Břeclav and surroundings (in Czech). *Archeologické rozhledy*, **72**: 523–572. <https://doi.org/10.35686/AR.2020.19>
- Dostál, B., 1968. K prehistorii a protohistorii Břeclavi (in Czech). In: *Břeclav. Dějiny města* (ed. M. Zemek): 9–44. Musejní spolek Brno, Břeclav.
- Dreibrodt, S., Lubos, C., Terhorst, B., Damm, B., Bork, H.-R., 2010. Historical soil erosion by water in Germany: scales and archives, chronology, research perspectives. *Quaternary International*, **222**: 80–95. <https://doi.org/10.1016/j.quaint.2009.06.014>
- Dresler, P., 2016. Břeclav – Pohansko VIII (in Czech). Industrial supportive environment of centrum or only village in the proximity of centre? Masaryk Univerzity, Brno.

- Dresler, P., Beran, V., 2019.** Agricultural tools of the Early Medieval Population of Pohansko near Břeclav (in Czech). *Památky archeologické*, **110**: 237–306.
- Dresler, P., Dreslerová, G., Doláková, N., Kočár, P., Kočárová, R., 2022.** Beaver as proof of the change of natural environment and economy of the first half of the 10th century AD. *Archaeologia Austriaca*, **106**: 117–136. <https://doi.org/10.1553/archaeologia106s117>
- Dreslerová, G., Hajnalová, M., Macháček, J., 2013.** Subsistenční strategie raně středověkých populací v dolním Podyjí. Archeozoologické a archeobotanické vyhodnocení nálezů z výzkumu Kostice – Zadní hrúd (2009–2011) (in Czech). *Archeologické rozhledy*, **65**: 825–850.
- Durand, M., 2006.** The problem of the transition from the Permian to the Triassic Series in southeastern France: comparison with other Peritethyan regions. *Geological Society Special Publications*, **265**: 281–296. <https://doi.org/10.1144/GSL.SP.2006.265.01.13>
- Elnicová, J., Kiss, T., Sipos, G., Faméra, M., Štojdl, J., Váchová, V., Matys Grygar, T., 2021.** A central European alluvial river under anthropogenic pressure: the Ohře River, Czechia. *Catena*, **201**: 105218. <https://doi.org/10.1016/j.catena.2021.105218>
- Erdtman, G., 1960.** The acetolysis method, a revised description. *Svensk Botanisk Tidskrift*, **54**: 561–564.
- Erkens, G., Hoffmann, T., Gerlach, R., Klostermann, J., 2011.** Complex fluvial response to Lateglacial and Holocene allogenic forcing in the Lower Rhine Valley (Germany). *Quaternary Science Reviews*, **30**: 611–627. <https://doi.org/10.1016/j.quascirev.2010.11.019>
- Folk, R.L., Ward, W., 1957.** Brazos River bar: a study in the significance of grain-size parameters. *Journal of Sedimentary Petrology*, **27**: 3–26.
- Gautier, E., Brunstein, D., Vauchel, P., Roulet, M., Fuertes, O., Guyot, J.L., Darozzes, J., Bourrel, L., 2007.** Temporal relations between meander deformation, water discharge and sediment fluxes in the floodplain of the Rio Beni (Bolivian Amazonia). *Earth Surface Processes and Landforms*, **32**: 230–248. <https://doi.org/10.1002/esp.1394>
- Gibbard, P.L., Lewin, J., 2002.** Climate and related controls on interglacial fluvial sedimentation in lowland Britain. *Sedimentary Geology*, **151**: 187–210. [https://doi.org/10.1016/S0037-0738\(01\)00253-6](https://doi.org/10.1016/S0037-0738(01)00253-6)
- Grygar, T., Nováková, T., Mihaljevič, M., Strnad, L., Světlík, I., Koptíková, L., Lisá, L., Brázdil, R., Máčka, Z., Stachoň, Z., Svitavská-Svobodová, H., Wray, D.S., 2011.** Surprisingly small increase of the sedimentation rate in the floodplain of Morava River in the Strážnické area, Czech Republic, in the last 1300 years. *Catena*, **86**: 192–207. <https://doi.org/10.1016/j.catena.2011.04.003>
- Havlíček, P., 2001.** Geology of the surroundings of the Great Moravian centre at Břeclav-Pohansko. *Zprávy o geologických výzkumech v roce 2000*, 71–73, Praha.
- Havlíček, P., 2004.** Geology of the river Dyje and Moravou confluence area (in Czech). In: Lužní les v Dyjsko-moravské nivě (eds. M. Hrib and E. Kordiovský): 11–19. Moraviapress, Břeclav.
- Havlíček, P., Smolíková, L., 2002.** Subrecent polygenetic pseudochernozem in the aeolian sands ("Barvínkův hrúd") at the confluence of the Dyje and Morava Rivers (s. Moravia) (in Czech). *Geologické výzkumy na Moravě a ve Slezsku*, **9**: 2–3.
- Havlíček, P., Břízová, E., Hošek, J., Sidorinová, T., 2016.** Geologický výzkum na soutoku Dyje, Kyjovky a Moravy. *Geoscience Research Reports*, **49**: 225–232.
- Hoffmann, T., Erkens, G., Gerlach, R., Klostermann, J., Lang, A., 2009.** Trends and controls of Holocene floodplain sedimentation in the Rhine catchment. *Catena*, **77**: 96–106. <https://doi.org/10.1016/j.catena.2008.09.002>
- Holliday, V.T., Gartner, W.G., 2007.** Methods of soil P analysis in archaeology. *Journal of Archaeological Science*, **34**: 301–333. <https://doi.org/10.1016/j.jas.2006.05.004>
- Houben, P., 2003.** Spatio-temporally variable response of fluvial systems to Late Pleistocene climate change: a case study from central Germany. *Quaternary Science Reviews*, **22**: 2125–2140. [https://doi.org/10.1016/S0277-3791\(03\)00181-1](https://doi.org/10.1016/S0277-3791(03)00181-1)
- IUSS Working Group WRB, 2014.** World reference base for soil resources 2014. In: *World Soil Resources Reports No. 106* (eds. P. Schad, P.C. van Huyssteen and E. Micheli). FAO, Rome.
- Jiříček, R., Seifert, P., 1990.** Paleogeography of the Neogene in the Vienna Basin and adjacent part of the foredeep. In: *Thirty Years of Geological Cooperation Between Austria and Czechoslovakia* (eds. D. Minaříková and H. Lobitzer): 89–105. Praha: ÚUG Special publication.
- Kadlec, J., Kocurek, G., Mohrig, D., Shinde, D.P., Murari, M.K., Varma, V., Stehlík, F., Beneš, V., Singhvi, A.K., 2015.** Response of fluvial, aeolian, and lacustrine systems to late Pleistocene to Holocene climate change, Lower Moravian Basin, Czech Republic. *Geomorphology*, **232**: 193–208. <https://doi.org/10.1016/j.geomorph.2014.12.030>
- Kadlec, J., Grygar, T., Světlík, I., Ettler, V., Mihaljevič, J.F., Diehl, S., Beske-Diehl, S., Svitavská-Svobodová, H., 2009.** Morava River floodplain development during the last millenium, Strážnické Pomoraví, Czech Republic. *The Holocene*, **19**: 499–510.
- Kalicki, T., 2006.** Reflection of climatic changes and human activity and their role in the Holocene evolution of central European valleys (in Polish with English summary). *Prace Geograficzne*, **204**.
- Komárek, J., Jankovská, V., 2001.** Review of the Green Algal Genus *Pediastrum*; Implication for Pollenanalytical Research. Gebrüder Borntraeger, Berlin.
- Kwiatkowska-Malina, J., 2018.** Functions of organic matter in polluted soils: the effect of organic amendments on phytoavailability of heavy metals. *Applied Soil Ecology*, **123**: 542–545. <https://doi.org/10.1016/j.apsoil.2017.06.021>
- Lespez, L., Clet-Pellerin, M., Limondin-Lozouet, N., Pastre, J.F., Fontugne, M., Marcigny, C., 2007.** Fluvial system evolution and environmental changes during the Holocene in the Mue valley (Western France). *Geomorphology*, **98**: 55–70. <https://doi.org/10.1016/j.geomorph.2007.02.029>
- Leigh, D.S., 2006.** Terminal Pleistocene braided to meandering transition in rivers of the South eastern USA. *Catena*, **66**: 155–160.
- Lewin, J., Macklin, M.G., 2010.** Floodplain catastrophes in the UK Holocene: messages for managing climate change. *Hydrological Process*, **24**: 2900–2911. <https://doi.org/10.1002/hyp.7704>
- Macháček, J., 2001.** Study to the pottery of the Great Moravia. *Metody, analýzy a syntézy, modely Masarykova univerzita, Brno*.
- Macháček, J., 2005.** Raně středověké centrum na Pohansku u Břeclavi: Munitio, palatium, Nebo emporium moravských panovníků? (in Czech). *Archeologické Rozhledy*, **57**: 100–138.
- Macháček, J., Doláková, N., Dresler, P., Havlíček, P., Hladilová, Š., Přichystal, A., Roszková, A., Smolíková, L., 2007.** Early Medieval centre at Pohansko near Břeclav and its natural environment (in Czech). *Archeologické Rozhledy*, **59**: 278–314.
- Macháček, J., Balcárková, A., Dresler, P., Přichystalová, R., Přišťáková, M., 2021.** Břeclav – Pohansko X. Settlement areal on the southeastern forefield (in Czech). *Archeologické výzkumy v letech 2008–2016*. Masarykova univerzita, Brno. <https://doi.org/10.5817/CZ.MUNI.M210-9893-2021>
- Macklin, M.G., Lewin, J., Woodward, J.C., 2012.** The fluvial record of climate change. *Philosophical Transactions of the Royal Society A*, **370**: 2143–2172. <https://doi.org/10.1098/rsta.2011.0608>
- Makaske, B., 2001.** Anastomosing rivers: a review of their classification, origin and sedimentary products. *Earth Science Reviews*, **53**: 149–196.
- Mazuch, M., 2013.** Velkomoravské keramické okruhy a tzv. mladší velkomoravský horizont v Mikulčicích (in Czech). *Archeologický ústav AV ČR, Brno*.
- Miall, A.D., 2006.** *The Geology of Fluvial Deposits. Sedimentary Facies, Basin Analysis, and Petroleum Geology*. Springer, Berlin.

- Mol, J., Vandenberghe, J., Kasse, C., 2000.** River response to variations of periglacial climate in mid-latitude Europe. *Geomorphology*, **33**: 131–148. [https://doi.org/10.1016/S0169-555X\(99\)00126-9](https://doi.org/10.1016/S0169-555X(99)00126-9).
- Moska, P., Bluszcz, A., Poreba, G., Tudyka, K., Adamiec, G., Szymak, A., Przybyła, A., 2021.** Luminescence dating procedures at the Gliwice Luminescence Dating Laboratory. *Geochronometria*, **48**: 1–15. <https://doi.org/10.2478/geochr-2021-0001>
- Mulder, T., Syvitski, J.P.M., 1995.** Turbidity currents generated at river mouths during exceptional discharges to the world oceans. *Journal of Geology*, **103**: 285–299. <https://www.jstor.org/stable/30071222>
- Nehyba, S., Dresler, P., Doláková, N., Kuda, F., Přišťáková, M., Šimík, J., Škojec, J., Kirchner, K., 2020.** The Early Medieval fluvial channel within the defence system of the Great Moravia Empire agglomeration Pohansko near Břeclav. *Geologické výzkumy na Moravě a ve Slezsku*, **27**: 54–61. <https://doi.org/10.5817/GVMS2020-13285>
- Nehyba, S., Dvořáková, M., Doláková, N., Dresler, P., 2018.** Quaternary deposits on the Northern bailey of the Pohansko site near Břeclav. *Geologické výzkumy na Moravě a ve Slezsku*, **25**: 34–40. <https://doi.org/10.5817/GVMS2018-1-2-34>
- Notebaert, B., Verstraeten, G., 2010.** Sensitivity of West and Central European river systems to environmental changes during the Holocene: a review. *Earth-Science Reviews*, **103**: 163–182. <https://doi.org/10.1016/j.earscirev.2010.09.009>
- Notebaert, B., Broothaerts, N., Verstraeten, G., 2018.** Evidence of anthropogenic tipping points in fluvial dynamics in Europe. *Global and Planetary Change*, **164**, 27–38. <https://doi.org/10.1016/j.gloplacha.2018.02.008>.
- Opravil, E., 1978.** Rostlinná společenstva v okolí Mikulčice v období předvelkomoravském a velkomoravském. (in Czech) *Archeologické rozhledy*, **30**: 67–75.
- Opravil, E., 1983.** Údolní niva v době hradištní (in Czech). *Studie Arc. Archeologický Ústav Československé akademie věd Brno, Praha*.
- Opravil, E., 2000.** Archäobotanische Funde aus dem Burgwall Pohansko bei Břeclav. In: *Studien zum Burgwall von Mikulčice* (ed. L. Poláček): 165–169. Archeologický ústav AV, Brno.
- Pettijohn, F.J., Potter, P.E., Siever, R., 1973.** *Sand and Sandstone*. Springer, Berlin.
- Petrík, J., Petr, L., Adameková, K., Přišťáková, M., Potůčková, A., Lendáková, Z., Fraćzek, M., Dresler, P., Macháček, J., Kalicki, T., Lisá, L., 2019.** Disruption in an alluvial landscape: Settlement and environment dynamics on the alluvium of the river Dyje at the Pohansko archaeological site (Czech Republic). *Quaternary International*, **511**: 124–139. <https://doi.org/10.1016/j.quaint.2018.04.013>
- Poláček, L., Hladík, M., 2014.** Archaeological excavation B 2012 of the filled-up riverbed and bridge No. 1 in Mikulčice. In: *Internationale Tagungen in Mikulčice X, Mikulčice River Archaeology* (ed. L. Poláček): 27–60. *New Interdisciplinary Research into Bridge no. 1*.
- Přišťáková, M., Milo, P., 2021.** Using geophysical survey as a tool for resolving issues of the structure of the built-up area of the early medieval centre at Pohansko near Břeclav, Czech Republic. *Archaeological Prospection*, **28**: 405–417. <https://doi.org/10.1002/arp.1811>
- Reille, M., 1995.** *Pollen et Spores d'Europe et d'Afrique du nord*. Marseille.
- Rulf, J., 1994.** Pravěké osídlení střední Evropy a niva (in Czech). In: *Archeologie a Krajinná Ekologie* (eds. J. Beneš and V. Brůna): 54–55. Nadace Projekt Sever, Most.
- Schlezinger, D.R., Howes, B.L., 2000.** Organic phosphorus and elemental ratios as indicators of prehistoric human occupation. *Journal of Archaeological Science*, **27**: 479–492. <https://doi.org/10.1006/jasc.1999.0464>
- Simons, D.B., Richardson, E.V., Nordin, C.L., 1965.** Sedimentary structures generated by flow in alluvial channels. *SEPM Special Publication 12*: 84–115. <https://doi.org/10.2110/pec.65.08.0034>
- Skolasińska, K., Nowak, B., 2018.** What factors affect the suspended sediment concentrations in rivers? A study of the upper Warta River (Central Poland). *River Research and Applications*, **34**: 112–123. <https://doi.org/10.1002/rra.3234>
- Starkel, L., Soja, R., Michczyńska, D.J., 2006.** Past hydrological events reflected in Holocene history of Polish rivers. *Catena*, **66**: 24–33. <https://doi.org/10.1016/j.catena.2005.07.008>
- Sumner, E., Amy, L., Talling, P.J., 2008.** Deposit structure and processes of sand deposition from a decelerating sediment suspension. *Journal of Sedimentary Research*, **78**: 529–547. <https://doi.org/10.2110/jsr.2008.062>
- Svobodová, H., 1990.** Vegetace jižní Moravy v druhé polovině prvního tisíciletí (in Czech). *Archeologické rozhledy*, **42**: 170–205.
- Toonen, W.H.J., Kleinhans, M.G., Cohen, K.M., 2012.** Sedimentary architecture of abandoned channel fills. *Earth Surface Process and Landforms*, **37**: 459–472. <https://doi.org/10.1002/esp.3189>
- Tucker, M., 1988.** *Techniques in Sedimentology*. Blackwell Science, Oxford.
- Vandenberghe, J., 2003.** Climate forcing of fluvial system development: an evolution of ideas. *Quaternary Science Reviews*, **22**: 2053–2060. [https://doi.org/10.1016/S0277-3791\(03\)00213-0](https://doi.org/10.1016/S0277-3791(03)00213-0)
- Vandenberghe, J., 2008.** The fluvial cycle at cold–warm–cold transitions in lowland regions: a refinement of theory. *Geomorphology*, **98**: 275–284. <https://doi.org/10.1016/j.geomorph.2006.12.030>
- Vandenberghe, J., Kasse, C., Bohncke, S., Kozarski, S., 1994.** Climate-related river activity at the Weichselian–Holocene transition: a comparative study of the Warta and Maas rivers. *Terra Nova*, **6**: 476–485. <https://doi.org/10.1111/j.1365-3121.1994.tb00891.x>
- Van Geel, B., Hallewas, D.P., Pals, J.P., 1983.** A Late Holocene deposit under Wetfiese Zeedijk near Enkhuizen (prov. of N-Holland, The Netherlands): paleoecological and archaeological aspects. *Review of Paleobotany and Palynology*, **38**: 269–335. [https://doi.org/10.1016/0034-6667\(83\)90026-X](https://doi.org/10.1016/0034-6667(83)90026-X)
- Vayssière, A., Rué, M., Recq, C., Gardère, P., Bozsó, E., Castanet, C., Virmoux, C., Gautier, E., 2019.** Lateglacial changes in river morphologies of northwestern Europe: an example of a smooth response to climate forcing (Cher River, France). *Geomorphology*, **342**: 20–36. <https://doi.org/10.1111/j.1365-3121.1994.tb00891.x>
- Walanus, A., Nalepka, D., 1999.** POLPAL. Program for counting pollen grains, diagrams plotting and numerical analysis. *Acta Palaeobotanica*, **2**: 659–661.
- Wallinga, J., 2008.** Optically stimulated luminescence dating of fluvial deposits: a review. *Boreas*, **31**: 303–322. <http://dx.doi.org/10.1111/j.1502-3885.2002.tb01076.x>
- Walker, R.G., James, N.P., 1992.** Facies Models. Response to sea level changes. *Geological Association of Canada, St. John's*. <https://doi.org/10.1002/gj.3350290317>
- Zieliński, T., Wiedera, M., 2020.** Anastomosing-to-meandering transitional river in sedimentary record: a case study from the Neogene of central Poland. *Sedimentary Geology*, **404**: 1–17. <https://doi.org/10.1016/j.sedgeo.2020.105677>